A Self-Adjoint Angular Flux Equation

J. E. Morel and J. M. McGhee
P.O. Box 1663, MS D409
Transport Methods Group, XTM
Los Alamos National Laboratory,
Los Alamos, NM 87545

Send proofs and page charges to:

Dr. J. E. Morel
Mail Stop D409
Los Alamos National Laboratory
Los AlamosΓ NM 87545

49 Pages – 0 Tables – 2 Figures

Abstract

The traditional second-order self-adjoint forms of the transport equation are the even-parity and odd-parity equations. A useful alternative to these equations exists in the form of a second-order self-adjoint equation that has the angular flux as its unknown. The numerical advantages and disadvantages of this equation are contrasted both theoretically and computationally with those of the even-parity and odd-parity equations.

1 Introduction

The even-parity and odd-parity transport equations are well-known second-order self-adjoint forms of the transport equation.[1] A computationally useful alternative to these equations exists in the form of a second-order self-adjoint equation that has the angular flux itself as the unknown rather than an even-parity or odd-parity component of the angular flux. We refer to this equation as the self-adjoint angular flux (SAAF) equation. Although it has previously appeared in the literatureΓ[2, 3] the SAAF equation is not well-known within the computational transport community. This may be due to the fact that the SAAF equation has always been previously presented within the context of variational approximations to the transport equation.[2, 3] Pomraning and Clark[2] first derived the SAAF equation from the first-order form of the transport equation using a purely algebraic techniqueΓ and then used the SAAF equation to generate a variational transport principle of the extremum type. This extremum principle was sought as an alternative to a saddle-point principle that they had previously obtained using the first-order form of the transport equation. They then used the extremum principle to obtain a more accurate form of diffusion theory. Pomraning and Clark[2] derived only the 1-D slab-geometry form of the SAAF equation and assumed that the cross sections were spatially independent. This assumption was necessitated by their particular approach to the derivation. While investigating generalized least-squares approximations to the first-order form of the transport equtaionΓ Ackroyd[3] showed that the SAAF equation is the Euler-Lagrange equation for a certain generalized least-squares functional. He derived the 3-D SAAF equation without any restriction on the spatial dependence of the cross-sections.

There are two primary purposes of this paper:

1. to show the SAAF equation can be derived from the first-order form of the transport equation using a purely algebraic technique that is simpler than than that of Pomraning and ClarkΓ[2] and yields the unrestricted 3-D equation derived by Ackroyd.[3].

2. to compare the SAAF equation with both the even-parity and odd-parity equations from a computational point of view.

The central point to be made is that the SAAF equation is an interesting and useful equation that deserves attention from the transport community. The remainder of this paper is organized as follows. First we list the computational advantages and disadvantages of the even-parity equationΓ the odd-parity equationΓ the SAAF equationΓ and the standard first-order transport equation. Next we derive the monoenergetic even-parityΓ odd-parityΓ and SAAF equations using very similar algebraic manipulations unrelated to variational methods. Boundary conditions for the SAAF equation are then derived and contrasted with those of the even-parity and odd-parity equations. Two multigroup forms of the

SAAF equation, which are suitable for solution via the P_n and S_n techniques respectively, are given next. A form of the SAAF equation that is suitable for void regions is then derived. Singularities that arise in the SAAF equation are discussed next. We then apply both S_n and P_n discretizations to the SAAF equation. It is shown that the P_n discretization can be formulated in two distinctly different ways. The first is equivalent to a least-squares approximation to the first-order transport equation, while the second is equivalent to the standard P_n approximation to the first-order transport equation. Results are then presented from a computational comparison of even-parity solutions, odd-parity solutions, averages of even-parity and odd-parity solutions, and SAAF solutions using a common discretization. Finally, we give conclusions and suggestions for future work.

2 Comparison of Equations

The traditional second-order self-adjoint forms of the transport equation are the even-parity and odd-parity equations.[1] These equations have both advantages and disadvantages relative the standard first-order form of the transport equation. For instance, a list of advantages follows:

1. The traditional self-adjoint equations can be solved on multidimensional finite-element spatial meshes using standard continuous finite-element discretization techniques.

Fundamental difficulties can arise on such meshes with the standard first-order form of the transport equation. In particularΓ a block lower-triangular ordering of the unknowns in the source iteration equations (with each block corresponding to the unknowns associated with a single spatial cell) may not exist because general finite-element meshes almost always contain slightly re-entrant cells. In additionΓ rigorous application of the discontinuous finite-element method is extremely complicated with re-entrant cells because solution discontinuities will sometimes occur on the interior of cell faces rather than occurring only along cell edges.

2. The application of continuous finite-element spatial discretizations results in matrix equations that are symmetric positive-definite (SPD.) Solution techniques for SPD systems are generally more efficient and robust than those for non-SPD systems. For instanceΓ the preconditioned conjugate-gradient method[4] is one of the most efficient and robust Krylov solution techniques in existenceΓ but it can only be applied to SPD systems.

3. The P_n equations are much more easily solved in a second-order self-adjoint form than in the first-order form because the flux moments are strongly coupled via the $\vec{\Omega} \cdot \vec{\nabla}$ operator.

A list of disadvantages follows:

1. The traditional self-adjoint S_n source iteration equations generate a general sparse matrix equation rather than a block lower-triangular matrix equation. Thus they cannot be solved using the standard sweeping technique used for the first-order S_n equations. This is not necessarily a disadvantage on general finite-element meshes because the standard sweeping technique may significantly degrade in efficiency when applied to the first-order S_n equations. HoweverΓ it often is a disadvantage on orthogonal meshes where the first-order S_n equations often can be very efficiently solved using the sweeping technique.

2. In multi-dimensionsΓ reflective and reflective-like boundary conditions result in fully implicit coupling between incoming and outgoing directions. In contrastΓ only one-way coupling occurs between incoming and outgoing directions with the standard first-order form of the transport equation. In particularΓ the outgoing directions appear in the equations for the incoming directionsΓ but incoming directions do not appear in the equations for the outgoing directions. The additional angular coupling associated with the traditional self-adjoint equations causes the diffusion-synthetic acceleration technique to degrade in effectiveness when applied to the S_n equations.[5] HoweverΓ it has no significant effect upon the P_n equations because the angular moments always couple at the boundaries regardless of whether the transport equation

is in a first-order or second-order form.

3. The full angular flux is difficult to numerically calculate because the even-parity and odd-parity flux components can be obtained with different orders of accuracy and are not spatially co-located. This arises because one component is always proportional to a gradient of the other.

4. Performing transport calculations with voids is problematic. The leakage terms in the even-parity and odd-parity equations contain the inverse of the total cross sectionΓ and thus become singular in a void. One can nonetheless define independent self-adjoint equations for the even-parity and odd-parity fluxes in a voidΓ but no relationship exists between these components. For exampleΓ one component is not proportional to the gradient of the other. Since the even and odd components couple at boundariesΓ one cannot satisfy boundary conditions without solving both equations.

5. Solving the steady-state odd-parity transport equation in a pure scattering region is problematic because a matrixΓ which must be inverted to obtain the relationship between the even-parity and odd-parity fluxesΓ becomes singular when $\sigma_s/\sigma_t = 1$. See Section 3.4 for more details.

The SAAF equation has all of the advantages previously listed for the traditional self-adjoint equations. It also has certain additional advantages:

1. The full angular flux is obtained when the SAAF equation is numerically solved rather than either the even-parity component or the odd-parity component alone. Thus the difficulties associated with constructing the full angular flux from numerical solutions to the traditional self-adjoint equations is avoided.

2. Because the full angular flux is present on the boundariesΓ reflective and reflective-like boundary conditions are much easier to implement. Most importantlyΓ incoming and outgoing directions couple in the SAAF equation in exactly the same manner that they couple in the *standard first-order transport equation.* This is particularly important when solving the SAAF equations with S_n angular discretization. The fully implicit coupling that occurs between incoming and outgoing directions at reflective boundaries with the even-parity and odd-parity S_n equations is avoided.

3. The SAAF equation (in an appropriate form) can be solved in a void because the full angular flux provides adequate information to satisfy the boundary conditions.

The SAAF equation shares only two disadvantages with the traditional self-adjoint equations:

1. The SAAF S_n source iteration equations generate a general sparse matrix equation rather than a block lower-triangular matrix equation. Thus they cannot be solved using the standard sweeping technique used for the first-order S_n equations.

2. Solving the steady-state SAAF equation in a pure scattering region is problematic. This property arises in the SAAF equation for the same reason that it arises in the odd-parity equation. See Section 3.4 for more details.

In additionΓ the SAAF equation has one significant disadvantage relative to the traditional self-adjoint equations. Because the full angular flux is the unknown in the SAAF equationΓ the angular domain is the full unit sphere. The angular domain associated with the traditional self-adjoint equations is a half of the unit sphere. Thus the SAAF equation requires twice as many angular unknowns for the same order of angular approximation as the traditional self-adjoint equations.

Solving the SAAF equation is closely related to solving *both* the even-parity and odd-parity equationsΓ but it is *not* equivalent. The even-parity and odd-parity equations are traditionally solved in a completely independent manner. We later show that solving the SAAF P_1 equations is equivalent to solving even-parity and odd-parity P_1 equations that are independent on the mesh interior but coupled at the boundaries.

3 Derivation of the Equations

We begin our derivations with the standard first-order form of the monoenergetic transport equation:[1]

$$\overrightarrow{\Omega} \cdot \overrightarrow{\nabla} \psi + \sigma_t \psi = S\psi + q \quad , \tag{1}$$

where $\overrightarrow{\Omega}$ is the directional variableΓψ is the angular fluxΓσ_t is the macroscopic total cross sectionΓS is the scattering operatorΓ and q is the inhomogeneous source. The scattering operator is assumed to be expressible as follows:

$$S\psi = \int_{4\pi} \sigma_s \left(\overrightarrow{\Omega}' \cdot \overrightarrow{\Omega} \right) \psi \left(\overrightarrow{\Omega}' \right) \, d\Omega' \quad , \tag{2}$$

where $\sigma_s \left(\overrightarrow{\Omega}' \cdot \overrightarrow{\Omega} \right)$ is the differential scattering cross-section. We first derive the even-parity and odd-parity equations. Substituting $-\overrightarrow{\Omega}$ for $\overrightarrow{\Omega}$ in Eq. (1)Γ adding the resulting equation to Eq. (1)Γ and dividing by 2Γ we obtain:

$$\overrightarrow{\Omega} \cdot \overrightarrow{\nabla} \psi^- + \sigma_t \psi^+ = S^+ \psi^+ + q^+ \quad , \tag{3}$$

where the even-parity flux is given by

$$\psi^+ = \frac{1}{2} \left(\psi(\overrightarrow{\Omega}) + \psi(-\overrightarrow{\Omega}) \right) \quad , \tag{4}$$

the odd-parity flux is given by

$$\psi^- = \frac{1}{2} \left(\psi(\overrightarrow{\Omega}) - \psi(-\overrightarrow{\Omega}) \right) \quad , \tag{5}$$

S^+ denotes the scattering operator restricted to the even-parity domainΓ andq^+ denotes the even-parity inhomogeneous sourceΓ which is defined in analogy with Eq. (4). Substituting $-\overrightarrow{\Omega}$ for $\overrightarrow{\Omega}$ in Eq. (1)Γ subtracting the resulting equation from Eq. (1)Γ and dividing by 2Γ we obtain:

$$\overrightarrow{\Omega} \cdot \overrightarrow{\nabla} \psi^+ + \sigma_t \psi^- = S^- \psi^- + q^- \quad , \tag{6}$$

where S^- denotes the scattering operator restricted to the odd-parity flux domainΓ andq^- denotes the odd-parity inhomogeneous source defined in analogy with Eq. (5). We obtain the even-parity transport equation by first solving Eq. (6) for ψ^- as follows:

$$\psi^- = -\left(\sigma_t - S^-\right)^{-1} \overrightarrow{\Omega} \cdot \overrightarrow{\nabla} \psi^+ + \left(\sigma_t - S^-\right)^{-1} q^- \quad , \tag{7}$$

and then substituting from Eq. (7) into the gradient term in Eq. (3):

$$-\overrightarrow{\Omega} \cdot \overrightarrow{\nabla} \left(\sigma_t - S^-\right)^{-1} \overrightarrow{\Omega} \cdot \overrightarrow{\nabla} \psi^+ + \left(\sigma_t - S^+\right) \psi^+ = q^+ - \overrightarrow{\Omega} \cdot \overrightarrow{\nabla} \left(\sigma_t - S^-\right)^{-1} q^- \quad . \tag{8}$$

We similarly obtain the the self-adjoint odd-parity transport equation by using Eq. (3) to solve to solve for ψ^+Γ and then substituting that expression into the gradient term in Eq. (6):

$$-\overrightarrow{\Omega} \cdot \overrightarrow{\nabla} \left(\sigma_t - S^+\right)^{-1} \overrightarrow{\Omega} \cdot \overrightarrow{\nabla} \psi^- + \left(\sigma_t - S^-\right) \psi^- = q^- - \overrightarrow{\Omega} \cdot \overrightarrow{\nabla} \left(\sigma_t - S^+\right)^{-1} q^+ \quad . \tag{9}$$

The derivation of the SAAF equation is very similar to the derivations of the even-parity and odd-parity equations. In particularΓ we use Eq. (1) to solve for ψ as follows:

$$\psi = -\left(\sigma_t - S\right)^{-1} \overrightarrow{\Omega} \cdot \overrightarrow{\nabla} \psi + \left(\sigma_t - S\right)^{-1} q \quad , \tag{10}$$

and then substitute from Eq. (10) into the gradient term in Eq. (1):

$$-\overrightarrow{\Omega} \cdot \overrightarrow{\nabla} \left(\sigma_t - S\right)^{-1} \overrightarrow{\Omega} \cdot \overrightarrow{\nabla} \psi + \left(\sigma_t - S\right) \psi = q - \overrightarrow{\Omega} \cdot \overrightarrow{\nabla} \left(\sigma_t - S\right)^{-1} q \quad . \tag{11}$$

Note that the basic structure of the SAAF equation is identical to that of the even-parity and odd-parity equations.

It is worthwhile to note that the SAAF equation can also be derived simply by adding the even-parity and odd-parity equations. HoweverΓ the derivation requires proof that $S\psi = S^{+}\psi^{+} + S^{-}\psi^{-}$.

3.1 Boundary Conditions

The SAAF boundary conditions for incoming directions are identical to those of the standard first-order transport equation. For instanceΓ at a boundary with an incoming fluxΓ the following condition is satisfied:

$$\psi(\overrightarrow{r}_b, \overrightarrow{\Omega}) = f(\overrightarrow{\Omega}) \quad , \overrightarrow{\Omega} \cdot \overrightarrow{n} < 0, \tag{12}$$

where $\overrightarrow{r}_b$ denotes a point on the boundary of the problem domainΓ $\overrightarrow{n}$ is the outward-directed boundary normalΓ and $f(\overrightarrow{\Omega})$ defines the incoming boundary flux. Note that a vacuum boundary condition is obtained by setting $f = 0$. The standard first-order transport equation does not require a boundary condition for outgoing directionsΓ but the SAAF equation does. We obtain one simply by requiring the SAAF solution to satisfy the first-order transport equation at the boundary:

$$\psi(\overrightarrow{r}_b, \overrightarrow{\Omega}) + (\sigma_t - S)^{-1}\, \overrightarrow{\Omega} \cdot \overrightarrow{\nabla}\psi(\overrightarrow{r}_b, \overrightarrow{\Omega}) = (\sigma_t - S)^{-1}\, q(\overrightarrow{r}_b, \overrightarrow{\Omega}) \qquad , \overrightarrow{\Omega} \cdot \overrightarrow{n} > 0. \quad (13)$$

Because the SAAf has second-order spatial derivativesΓ it admits more solutions than the first-order form of the transport equation. A natural way to ensure that spurious solutions to the SAAF equation are eliminated is to make the SAAf solution satisfy the forst-order equation on outflow boundaries.

Equation (12) also applies for a reflective condition if we define the incoming flux as follows:

$$f(\overrightarrow{\Omega}) = \psi(\overrightarrow{\Omega}') \qquad , \quad (14)$$

where $\overrightarrow{\Omega}$ is mapped to $\overrightarrow{\Omega}'$ via specular reflection. Thus the outgoing fluxes appear in the reflective boundary condition for the incoming fluxes. Equation (13) also applies for a reflective conditionΓ but it requires no modification. Thus the incoming fluxes do not appear in the reflective boundary condition for the outgoing fluxes. This type of "one-way" coupling at reflective boundaries is identical to that of the standard first-order form of the transport equation. This property is extremely important for S_n calculations because it ensures independent source iteration equations for each direction whenever the standard first-order S_n equations display such independence. The two-way coupling between directions which occurs at reflective boundaries with the even-parity and odd-parity equations can lead to significant degradation of the source iteration convergence rate even when diffusion-synthetic acceleration is applied.[5]

3.2 Source Iteration Forms

In most instancesΓ energy-dependent versions of the operator $(\sigma_t - S)^{-1}$ are not self-adjoint. If this operator is not self-adjointΓ the SAAF equation is not self-adjointΓ and the discretized SAAF equations will no longer be symmetric positive-definite (SPD). This would seem to imply that the sophisticated solution techniques that can be applied only to SPD systems could no longer be applied to the SAAF equation. FortunatelyΓ this potential difficulty can be avoided by using the multigroup energy treatment in conjunction with source iteration. Source iteration for the between-group component of the scattering source is routinely used in both P_n and S_n calculationsΓ and it is only this component that is not self-adjoint. For instanceΓ the multigroup version of Eq. (11) appropriate for P_n calculations can be written as follows:

$$-\overrightarrow{\Omega} \cdot \overrightarrow{\nabla} \left(\sigma_t - S_d\right)^{-1} \overrightarrow{\Omega} \cdot \overrightarrow{\nabla} \psi + \left(\sigma_t - S_d\right) \psi = S_o \psi + q - \overrightarrow{\Omega} \cdot \overrightarrow{\nabla} \left(\sigma_t - S_d\right)^{-1} \left(S_o \psi + q\right) \ , \quad (15)$$

where S_d denotes the within-group block of the multigroup scattering matrixΓ andS_o denotes the between-group block of the multigroup scattering matrix. Note that the multigroup notation for matrices and vectors is suppressed in Eq. (15) for simplicity. There is no difficulty solving Eq. (15) via source iteration because the operator on the left side of Eq. (15) is self-adjoint and positive-definite. The monoenergetic version of Eq. (11) appropriate for S_n calculations can be written as follows:

$$-\vec{\Omega} \cdot \vec{\nabla} \frac{1}{\sigma_t} \vec{\Omega} \cdot \vec{\nabla} \psi + \sigma_t \psi = S\psi + q - \vec{\Omega} \cdot \vec{\nabla} \frac{(S\psi + q)}{\sigma_t} \quad . \tag{16}$$

The form of Eq. (16) remains unchanged in the multigroup case. There is no problem solving Eq. (16) via source iteration because the operator on the left side of Eq. (16) is self-adjoint and positive definite.

Diffusion-synthetic acceleration can easily be applied to Eq. (16) using the SAAF P_1 equations as the low-order operator for the SAAF S_n equations. Since they are both second-order equationsΓ one can apply the same finite-element spatial approximation to these equations and thereby achieve consistency between the high-order and low-order operators. The approach is analogous to that developed by Morel and McGhee.[5] for the even-parity S_n equations.

3.3 Void Forms of the SAAF Equation

To obtain an SAAF equation appropriate for a voidΓ we first take Eq. (11) and assume a purely absorbing medium with a spatially constant cross-section:

$$-\overrightarrow{\Omega} \cdot \overrightarrow{\nabla} \frac{1}{\sigma_a} \overrightarrow{\Omega} \cdot \overrightarrow{\nabla} \psi + \sigma_a \psi = 0 \quad . \tag{17}$$

Since the cross-section is constantΓ we can move it through the gradient term and multiply the equation by σ_a:

$$-\overrightarrow{\Omega} \cdot \overrightarrow{\nabla} \overrightarrow{\Omega} \cdot \overrightarrow{\nabla} \psi + \sigma_a^2 \psi = 0 \quad . \tag{18}$$

FinallyΓ taking the limit as$\sigma_a \to 0$Γ we obtain the desired void equation:

$$-\overrightarrow{\Omega} \cdot \overrightarrow{\nabla} \overrightarrow{\Omega} \cdot \overrightarrow{\nabla} \psi = 0 \quad . \tag{19}$$

Following an analogous procedureΓ we obtain the following even-parity and odd-parity void equations respectively:

$$-\overrightarrow{\Omega} \cdot \overrightarrow{\nabla} \overrightarrow{\Omega} \cdot \overrightarrow{\nabla} \psi^{+} = 0 \quad , \tag{20}$$

and

$$-\overrightarrow{\Omega} \cdot \overrightarrow{\nabla} \overrightarrow{\Omega} \cdot \overrightarrow{\nabla} \psi^{-} = 0 \quad . \tag{21}$$

Equations (20) and (21) cannot be solved independently because the even-parity and odd-parity fluxes couple at boundariesΓ and these fluxes are no longer related by Eqs. (3) and

(6). Thus one must simultaneously solve Eqs. (20) and (21) in order to have the information required by both of these equations at the boundaries.

For instanceΓ let us first consider boundary conditions for the non-void even-parity equation and demonstrate why Eqs. (8) and (9) can be solved independently. The vacuum boundary condition for the first-order transport equation is

$$\psi(\overrightarrow{\Omega}) = 0 \qquad , \overrightarrow{\Omega} \cdot \overrightarrow{n} < 0, \tag{22}$$

To get the corresponding boundary condition for Eq. (8)Γ we first sum Eqs. (4) and (5) to obtain

$$\psi(\overrightarrow{\Omega}) = \psi^{+}(\overrightarrow{\Omega}) + \psi^{-}(\overrightarrow{\Omega}) \qquad . \tag{23}$$

Next we substitute from Eq. (23) into Eq. (22):

$$\psi^{+}(\overrightarrow{\Omega}) + \psi^{-}(\overrightarrow{\Omega}) = 0 \qquad , \overrightarrow{\Omega} \cdot \overrightarrow{n} < 0. \tag{24}$$

In order to solve Eq. (8) without solving Eq. (9)Γ we must express the odd-parity flux in Eq. (24) in terms of the even-parity flux. This is done via Eq. (7). Substituting from Eq. (7) into Eq. (24)Γ we obtain a boundary condition that contains only the even-parity flux:

$$\psi^{+}(\overrightarrow{\Omega}) - \left(\sigma_t - S^{-}\right)^{-1} \overrightarrow{\Omega} \cdot \overrightarrow{\nabla} \psi^{+} + \left(\sigma_t - S^{-}\right)^{-1} q^{-} = 0 \qquad , \overrightarrow{\Omega} \cdot \overrightarrow{n} < 0. \tag{25}$$

Equation (24) remains valid in a voidΓ but Eq. (7) no longer relates the even-parity and odd-parity fluxes. ConsequentlyΓ one cannot eliminate ψ^- from Eq. (24)Γ so Eqs. (20) and (21) must be solved simultaneously.

The boundary condition for Eq. (19) for incoming directions is identical to that for Eq. (11):

$$\psi(\overrightarrow{r}_b, \overrightarrow{\Omega}) = f(\overrightarrow{\Omega}) \qquad , \overrightarrow{\Omega} \cdot \overrightarrow{n} < 0, \tag{26}$$

In analogy with Eq. (13)Γ we use the first-order form of the transport equation to obtain the boundary condition for outgoing directions:

$$\overrightarrow{\Omega} \cdot \overrightarrow{\nabla} \psi(\overrightarrow{r}_b, \overrightarrow{\Omega}) = 0 \qquad , \overrightarrow{\Omega} \cdot \overrightarrow{n} > 0, \tag{27}$$

There are two notable difficulties that can arise when numerically solving Eq. (19). Unlike the non-void SAAF equationΓ Eq. (19) does not constitute a statement of particle conservation. While it is true that an analytic solution to Eq. (19) (with appropriate boundary conditions) will solve the first-order form of the transport equation and thus satisfy particle conservationΓ it is not clear that numerical solutions to Eq. (19) can be made to satisfy particle conservation. By definitionΓ a numerical approximation is conservative if it preserves the integral of the standard transport equation over the problem domain. In a voidΓ this requirement takes the following form:

$$\int \overrightarrow{\Omega} \cdot \overrightarrow{\nabla} \tilde{\psi} \, dP = 0 \qquad , \tag{28}$$

where $\tilde{\psi}$ denotes the approximate solution for ψ. This integral can either be satisfied rigorously via finite-element methods or it can be satisfied in a discrete sense.

Let us contrast the conservative nature of the non-void form of the SAAF equationΓ Eq. (11)Γ with the non-conservative nature of the void formΓ Eq. (19). Equation (11) represents an expression of particle conservation because

$$\psi = -\left(\sigma_t - S\right)^{-1} \overrightarrow{\Omega} \cdot \overrightarrow{\nabla} \psi + \left(\sigma_t - S\right)^{-1} q \quad . \tag{29}$$

Thus Eq. (11) is equivalent to the first-order equation via substitutionΓ i.e.Γ substituting Eq. (29) into Eq. (19) yields the first-order form of the transport equation. ConsequentlyΓ integrating Eq. (11) over the problem domain is equivalent to integrating the first-order form of the transport equation over that domain. HoweverΓ Equation (19) does not represent a statement of particle conservation because

$$\psi \neq -\overrightarrow{\Omega} \cdot \overrightarrow{\nabla} \psi \quad . \tag{30}$$

Thus Eq. (19) is not equivalent to the first-order equation via substitutionΓ and integrating Eq. (19) over the problem domain is not equivalent to integrating the first-order form of the transport equation over that domain.

NonethelessΓ the question naturally arises as to whether it is possible to satisfy Eq. (28) via Eq. (19) in some indirect manner. In 1-D slab geometryΓ the void solution for the angular flux is a constant. Hence almost any consistent discretization of Eq. (19) will result in the exact (and thus conservative) solution. However, in any other geometry, one cannot generally expect to obtain exact void solutions. For this general case, an indirect means of satisfying Eq. (28) via Eq. (19) is not apparent to us. However, we cannot prove that such a means does not exist. This is a subject for future research.

In a numerical problem containing both void and non-void regions, one must define a method for interfacing Eqs. (11) and (19). There are many possible ways to do this. The challenge is to find an interface technique that is accurate and retains an SPD coefficient matrix. Manteuffel and Ressel[7] have developed a least-squares method for solving the transport equation that is closely related to solving the SAAF equation. Although they did not perform any computations with void regions, their formalism admits such regions. Furthermore, their formalism yields an SPD coefficient matrix in calculations with both void and non-void regions. A study of the solution of the SAAF equation in voids is beyond the scope of this paper, but it is clear that this is an important area for future research.

3.4 Singularities of the SAAF Equation

As previously noted, both the the odd-parity and SAAF equations become singular in the limit as $\sigma_s/\sigma_t \to 1$. These singularities arise from the $(\sigma_t - S^+)^{-1}$ and $(\sigma_t - S)^{-1}$ matrices. As shown in the Appendix the matrices S^+ and S are diagonal in the spherical-harmonic basis. For instanceΓ in the 1-D monoenergetic caseΓ

$$S = \mathrm{diag}(\sigma_0, \sigma_1, \sigma_2, \ldots) \quad , \tag{31}$$

and

$$S^+ = \mathrm{diag}(\sigma_0, \sigma_2, \sigma_4, \ldots) \quad , \tag{32}$$

where σ_l denotes the l'th Legendre moment of the scattering cross-section. It is evident from Eqs. (31) and (32) that

$$(\sigma_t - S)^{-1} = \mathrm{diag}(\frac{1}{\sigma_t - \sigma_0}, \frac{1}{\sigma_t - \sigma_1}, \frac{1}{\sigma_t - \sigma_2}, \ldots) \quad , \tag{33}$$

and

$$(\sigma_t - S^+)^{-1} = \mathrm{diag}(\frac{1}{\sigma_t - \sigma_0}, \frac{1}{\sigma_t - \sigma_2}, \frac{1}{\sigma_t - \sigma_4}, \ldots) \quad . \tag{34}$$

In a purely scattering mediumΓ $\sigma_t - \sigma_0 = 0$. Thus it can seen from Eqs. (33) and (34) that a singularity arises in the first element of both matrices. This singularity can be avoided by solving the source-iteration form of the SAAF equation given in Eq. (16). UnfortunatelyΓ this is not a very practical solution since the source iteration process can converge arbitrarily slowly in a purely scattering medium. The use of diffusion-synthetic acceleration (DSA) to avoid the convergence difficulties immediately comes to mindΓ[5] but it must be remembered that the the odd-parity and SAAF P_1 equations are themselves singular in a purely scattering medium. Thus a straightforward form of DSA is not possible.

Adams has shown that an asymptotic diffusion equation can be derived from the odd-parity S_n equations in 1-D slabsΓ[6] and further that it can be used to produce an effective DSA scheme. This suggests that a similar approach might be possible for the SAAF equation. An investigation of the asymptotic properties of spatially-discrete SAAF equations in the thick-diffusion limit is beyond the scope of this paper. HoweverΓ we have performed a preliminary study that shows that the 1-D slab-geometry SAAF S_n equations with lumped linear-continuous finite-element spatial discretization produce independent vertex-centered and cell-centered diffusion equations in the thick diffusion limit. We intend to investigate the use of these equations in a DSA scheme for the SAAF S_n equations in the near future.

4 S_n Discretization

The SAAF equation is trivially discretized via the S_n approximation. In particularΓ we obtain the following monoenergetic 1-D slab-geometry S_N equations:

$$-\mu_m^2 \frac{\partial}{\partial x} \frac{1}{\sigma_t} \frac{\partial}{\partial x} \psi_m + \sigma_t \psi_m = S\psi_m + q_m - \mu \frac{\partial}{\partial x} \frac{S\psi_m + q_m}{\sigma_t} \qquad \text{, m=1ΓN} \tag{35}$$

where

$$S\psi_m = \sum_{l=0}^{L} (2l+1) \sigma_l \phi_l P_l(\mu_m) \qquad \text{, m=1ΓN} \tag{36}$$

$$\phi_l = \sum_{m=1}^{M} \psi_m P_l(\mu_m) w_m \qquad \text{, l=0ΓL} \tag{37}$$

and where m is the angular indexΓN denotes the quadrature orderΓL denotes the degree of the cross-section expansion$\Gamma P_l(x)$ denotes the Legendre polynomial of degree $l\Gamma w_m$ denotes the quadrature weight associated with the m'th quadrature cosine$\Gamma\mu_m$.

For reasons that become clear in our discussion of P_n discretizationsΓ it is significant to note that we can obtain the above equations in two distinct ways:

- Directly apply the S_n discretization to the SAAF equation.
- Apply the S_n discretization to the first-order form of the transport equationΓ and then *derive* an SAAF discretization via the same algebraic procedure by which the SAAF equation is derived from the first-order form of the transport equation.

We refer to the former as the direct procedure and to the latter as the indirect procedure. Because both of these procedures produce the same equationsΓ it follows that our SAAF S_n equations are completely equivalent to the standard S_n equations for the first-order form of the transport equation. We stress that this equivalence necessarily holds only for the spatially-analytic equations.

The spatial discretization technique that we define here is quite simple and represents a lumped version of the linear-continuous finite-element method.[8] HoweverΓ we derive it from a purely finite-difference viewpoint for the sake of simplicity. As is customaryΓ we denote cell-edge quantities with half-integral indices and cell-center quantities with integral indices.

Each spatial cell is assumed to contain a homogeneous materialΓ but materials may differ between cells. Our equations contain both cell-center and cell-edge unknowns.

The equation for the angular flux at cell-center i and direction m represents a balance equation for the first-order form of the transport equation over the interval $[x_{i-\frac{1}{2}}, x_{i+\frac{1}{2}}]$:

$$\mu_m \left(\psi_{i+\frac{1}{2},m} - \psi_{i-\frac{1}{2},m}\right) + \sigma_{t,i}\psi_{i,m}\Delta x_i = Q_{i,m}\Delta x_i \quad , \tag{38}$$

where

$$\Delta x_i = x_{i+\frac{1}{2}} - x_{i-\frac{1}{2}} \quad , \tag{39}$$

and

$$Q_{i,m} = S\psi_{i,m} + q_{i,m} \quad . \tag{40}$$

The equation for the angular flux at cell-edge $i + \frac{1}{2}$ and direction m represents a balance equation for the first-order form of the transport equation over the interval $[x_i, x_{i+1}]$:

$$\mu_m \left(\psi_{i+1,m} - \psi_{i,m}\right) + \sigma_{t,i+\frac{1}{2}}\psi_{i+\frac{1}{2},m}\Delta x_{i+\frac{1}{2}} = Q_{i+\frac{1}{2},m}\Delta x_{i+\frac{1}{2}} \quad , \tag{41}$$

where

$$\sigma_{t,i+\frac{1}{2}} = \frac{\sigma_{t,i}\Delta x_i + \sigma_{t,i+1}\Delta x_{i+1}}{\Delta x_i + \Delta x_{i+1}} \quad , \tag{42}$$

$$\Delta x_{i+\frac{1}{2}} = \frac{1}{2}\left(\Delta x_i + \Delta x_{i+1}\right) \quad . \tag{43}$$

We now obtain an interior-mesh discretization for the SAAF equation by first solving Eq. (38) for $\psi_{i,m}$:

$$\psi_{i,m} = -\frac{\mu_m}{\sigma_{t,i}\Delta x_i}\left(\psi_{i+\frac{1}{2},m} - \psi_{i-\frac{1}{2},m}\right) + \frac{Q_{i,m}}{\sigma_{t,i}} \quad , \tag{44}$$

and then using Eq. (44) to eliminate the cell-center fluxes from Eq. (41):

$$\begin{gathered} -\tfrac{\mu_m^2}{\sigma_{t,i+1}\Delta x_{i+1}}\left(\psi_{i+\frac{3}{2},m} - \psi_{i+\frac{1}{2},m}\right) + \tfrac{\mu_m^2}{\sigma_{t,i}\Delta x_i}\left(\psi_{i+\frac{1}{2},m} - \psi_{i-\frac{1}{2},m}\right) + \\ \sigma_{t,i+\frac{1}{2}}\psi_{i+\frac{1}{2},m}\Delta x_{i+\frac{1}{2}} = Q_{i+\frac{1}{2},m}\Delta x_{i+\frac{1}{2}} - \mu_m\left(\tfrac{Q_{i+1,m}}{\sigma_{t,i+1}} - \tfrac{Q_{i,m}}{\sigma_{t,i}}\right) \quad . \end{gathered} \tag{45}$$

Equation (45) applies to all of the cell-edge angular fluxes except those on the left $(i = \frac{1}{2})$ and right $(i = I + \frac{1}{2})$ boundaries.

The equation for $\psi_{\frac{1}{2},m}\Gamma$ takes the form of a balance equation over the interval $[x_{\frac{1}{2}}, x_1]$:

$$\mu_m\left(\psi_{1,m} - \psi_{L,m}\right) + \sigma_{t,1}\psi_{\frac{1}{2},m}\frac{\Delta x_1}{2} = Q_{\frac{1}{2},m}\frac{\Delta x_1}{2} \quad , \tag{46}$$

where $\psi_{L,m}$ takes on different values for incoming and outgoing directions:

$$\psi_{L,m} = f_m \qquad , \mu_m > 0, \tag{47}$$

$$\psi_{L,m} = \psi_{\frac{1}{2},m} \qquad , \mu_m < 0, \tag{48}$$

where for a source condition f_m denotes the incident fluxΓ for a vacuum condition $f_m = 0\Gamma$ and for a reflective condition $f_m = \psi_{\frac{1}{2}}(-\mu_m)$. Note that Eq. (47) is itself compatible with Eq. (12)Γ while Eq. (46) together with Eq. (48) is compatible as a whole with Eq. (13).

Using Eq. (44) to eliminate $\psi_{1,m}$ from Eq. (46)Γ we obtain the SAAF discretization for the left boundary vertex flux:

$$-\frac{\mu_m^2}{\sigma_{t,1}\Delta x_1}\left(\psi_{\frac{3}{2},m}-\psi_{\frac{1}{2},m}\right)-\mu_m\psi_{L,m}+\sigma_{t,1}\psi_{\frac{1}{2},m}\frac{\Delta x_1}{2}=Q_{\frac{1}{2},m}\frac{\Delta x_1}{2}-\mu_m\frac{Q_{1,m}}{\sigma_{t,1}} \quad , \tag{49}$$

As previously notedΓ we have used a lumped version of the linear-continuous finite-element method to spatially discretize the SAAF S_n equations. The standard finite-element equations are "lumped" by replacing three-point cell-edge removal and source terms with one-point terms. This results in a more robust (i.eΓ more positive) discretization at the cost of accuracy. Although both the lumped and standard equations are second-order accurateΓ the error is nonetheless larger for the lumped scheme in the thin-mesh limit. To obtain the standard finite-element S_n discretization from the lumped discretizationΓ make the following substitutions in Eq. (45):

$$\sigma_{t,i+\frac{1}{2}}\psi_{i+\frac{1}{2},m}\Delta x_{i+\frac{1}{2}}\rightarrow\sigma_{t,i}\left(\frac{1}{3}\psi_{i-\frac{1}{2},m}+\frac{2}{3}\psi_{i+\frac{1}{2},m}\right)\frac{\Delta x_i}{2}+\sigma_{t,i+1}\left(\frac{2}{3}\psi_{i+\frac{1}{2},m}+\frac{1}{3}\psi_{i+\frac{3}{2},m}\right)\frac{\Delta x_{i+1}}{2}, \tag{50}$$

$$Q_{i+\frac{1}{2},m}\Delta x_{i+\frac{1}{2}}\rightarrow\left(\frac{1}{3}Q_{i-\frac{1}{2},m}+\frac{2}{3}Q_{i+\frac{1}{2},m}\right)\frac{\Delta x_i}{2}+\left(\frac{2}{3}Q_{i+\frac{1}{2},m}+\frac{1}{3}Q_{i+\frac{3}{2},m}\right)\frac{\Delta x_{i+1}}{2} \quad , \tag{51}$$

and the following substitutions in Eq. (46):

$$\sigma_{t,1}\psi_{\frac{1}{2},m}\frac{\Delta x_1}{2}\rightarrow\sigma_{t,1}\left(\frac{2}{3}\psi_{\frac{1}{2},m}+\frac{1}{3}\psi_{\frac{3}{2},m}\right)\frac{\Delta x_1}{2} \quad , \tag{52}$$

$$Q_{\frac{1}{2},m}\frac{\Delta x_1}{2}\rightarrow\left(\frac{2}{3}Q_{\frac{1}{2},m}+\frac{1}{3}Q_{\frac{3}{2},m}\right)\frac{\Delta x_1}{2} \quad . \tag{53}$$

FinallyΓ we note that we explicitly define the inhomogeneous sources only at the vertices and calculate the cell-center sources by averaging the adjacent vertex sources:

$$q_{i,m} = \frac{1}{2}\left(q_{i-\frac{1}{2},m} + q_{i+\frac{1}{2},m}\right) \quad . \tag{54}$$

We stress that this is *not* done for the scattering sources. The cell-center scattering sources must be calculated with the cell-center fluxes for consistency.

5 P_n Discretization

In the previous section we described direct and indirect procedures for obtaining the S_n discretization for the SAAF equation. Both procedures result in the same S_n discretizationΓ but they result in *different* P_n discretizations. To demonstrate thisΓ we first take the indirect approach. In particularΓ we assume a P_1 expansion for the angular flux in the first-order form of the transport equation and then take P_0 and P_1 moments of that equation. The following respective equations are obtained:

$$\frac{\partial}{\partial x}\phi_1 + (\sigma_t - \sigma_0)\,\phi_0 = \varsigma_0 \quad , \tag{55}$$

$$\frac{1}{3}\frac{\partial}{\partial x}\phi_0 + (\sigma_t - \sigma_1)\,\phi_1 = \varsigma_1 \quad , \tag{56}$$

where ς_l denotes the l'th Legendre moment of the inhomogeneous source. Using Eq. (56) to eliminate ϕ_1 from Eq. (55)Γ we obtain

$$-\frac{\partial}{\partial x}\frac{1}{3\left(\sigma_t-\sigma_1\right)}\frac{\partial}{\partial x}\phi_0+\left(\sigma_t-\sigma_0\right)\phi_0=\varsigma_0-\frac{\partial}{\partial x}\frac{\varsigma_1}{\left(\sigma_t-\sigma_1\right)} \quad , \tag{57}$$

Using Eq. (55) to eliminate ϕ_0 from Eq. (56)Γ we obtain

$$-\frac{\partial}{\partial x}\frac{1}{3\left(\sigma_t-\sigma_0\right)}\frac{\partial}{\partial x}\phi_1+\left(\sigma_t-\sigma_1\right)\phi_1=\varsigma_1-\frac{\partial}{\partial x}\frac{\varsigma_0}{3\left(\sigma_t-\sigma_0\right)} \quad . \tag{58}$$

Equations (57) and (58) represent a P_1 approximation to the SAAF equation.

If we use the direct approachΓ i.e.Γ assume a P_1 expansion for the angular fluxΓ substitute it into the SAAF equationΓ and take P_0 and P_1 momentsΓ respectivelyΓ we still obtain Eq. (57)Γ but Eq. (58) is replaced with

$$-\frac{\partial}{\partial x}\left[\frac{1}{3\left(\sigma_t-\sigma_0\right)}+\frac{4}{15\left(\sigma_t-\sigma_2\right)}\right]\frac{\partial}{\partial x}\phi_1+\left(\sigma_t-\sigma_1\right)\phi_1=\varsigma_1-\frac{\partial}{\partial x}\frac{\varsigma_0}{3\left(\sigma_t-\sigma_1\right)} \quad . \tag{59}$$

Since Eqs. (57) and (58) represent the standard P_1 equationsΓ the question naturally arises as to what Eqs. (57) and (59) represent.

To answer this questionΓ we must further consider the connection between the SAAF equation and least-squares approximations to the first-order form of the transport equation. We begin the discussion by noting that if $\sigma_t \neq \sigma_0$Γ the operatorΓ $(\sigma_t - S)^{-1}$Γ has a diagonal representation with strictly positive elements (e.g.Γ see the Appendix). Thus this operator has a square root, $(\sigma_t - S)^{-\frac{1}{2}}$. Furthermore, $(\sigma_t - S)^{-\frac{1}{2}}$ is self-adjoint with respect to the standard inner product:

$$
\begin{aligned}
\langle (\sigma_t - S)^{-\frac{1}{2}} u, h \rangle_s &= \int \int_{4\pi} \left[(\sigma_t - S)^{-\frac{1}{2}} u \right] h \, d\Omega \, dV \quad , \\
&= \int \int_{4\pi} u \, (\sigma_t - S)^{-\frac{1}{2}} h \, d\Omega \, dV \quad , \\
&= \langle u, (\sigma_t - S)^{-\frac{1}{2}} h \rangle_s \quad , \qquad (60)
\end{aligned}
$$

where u and h denote any two square-integrable functions, and the spatial integral is taken over all space. Thus we can use this operator to define the following "operator-weighted" inner product:

$$
\begin{aligned}
\langle u, h \rangle &= \int \int_{4\pi} \left[(\sigma_t - S)^{-\frac{1}{2}} u \right] \left[(\sigma_t - S)^{-\frac{1}{2}} h \right] \, d\Omega \, dV \quad , \\
&= \int \int_{4\pi} u \, (\sigma_t - S)^{-1} h \, d\Omega \, dV \quad , \\
&= \int \int_{4\pi} \left[(\sigma_t - S)^{-1} u \right] h \, d\Omega \, dV \quad , \\
&= \int \int_{4\pi} h \, (\sigma_t - S)^{-1} u \, d\Omega \, dV \quad , \qquad (61)
\end{aligned}
$$

where, as in Eq. (60), u and h denote any two square-integrable functions, and the spatial integral is taken over all space. Let $\mathcal{L}$ denote the first-order monoenergetic transport operator, i.e.,

$$
\mathcal{L}\psi = \overrightarrow{\Omega} \cdot \overrightarrow{\nabla} \psi + \sigma_t \psi - S\psi \quad . \qquad (62)
$$

The adjoint transport operator corresponding to the inner product that we have defined,

$\mathcal{L}^\dagger$Γ satisfies

$$\langle \mathcal{L}^\dagger u, h \rangle = \langle u, \mathcal{L} h \rangle \quad , \tag{63}$$

for all u and hΓ and takes the following form:

$$\mathcal{L}^\dagger u = -\left(\sigma_t - S\right) \overrightarrow{\Omega} \cdot \overrightarrow{\nabla} \left(\sigma_t - S\right)^{-1} u + \left(\sigma_t - S\right) u \quad . \tag{64}$$

Note that the definition of the adjoint transport operator depends upon the inner productΓ i.e.Γ a different inner product will give rise to a different adjoint transport operator. It is easily verified that the SAAF equation can be expressed as follows:

$$\left(\sigma_t - S\right)^{-1} \mathcal{L}^\dagger \mathcal{L} \psi = \left(\sigma_t - S\right)^{-1} \mathcal{L}^\dagger q \quad . \tag{65}$$

NowΓ let us define the following generalized least-squares functional for the first-order transport equation:

$$\Gamma = \langle \mathcal{L}\psi - q, \mathcal{L}\psi - q \rangle \quad , \tag{66}$$

Let us further assume a spherical-harmonic expansion for the angular flux:

$$\psi(\overrightarrow{r}, \overrightarrow{\Omega}) = \sum_{l=0}^{L} \sum_{m=-l}^{l} \frac{2l+1}{4\pi} \phi_l^m(\overrightarrow{r}) Y_l^m(\overrightarrow{\Omega}) \quad , \tag{67}$$

where Y_l^m denotes the spherical-harmonic function of order l and degree m as defined in the AppendixΓ and ϕ_l^m denotes the corresponding spherical-harmonic moment of the angular flux:

$$\phi_l^m = \int_{4\pi} \psi\left(\overrightarrow{\Omega}\right) Y_l^m\left(\overrightarrow{\Omega}\right) d\Omega \quad , \tag{68}$$

To minimize $\Gamma\Gamma$ we first make the following substitution:

$$\phi_l^m(\overrightarrow{r}) \rightarrow \phi_l^m(\overrightarrow{r}) + \epsilon_l^m v_l^m(\overrightarrow{r}) \qquad , \tag{69}$$

where ϵ_l^m is a parameter and $v_l^m(\overrightarrow{r})$ is an arbitrary square-integrable function. Then we require that

$$\left.\frac{\partial \Gamma}{\partial \epsilon_k^j}\right|_{\epsilon_k^j=0} = 0 \qquad \text{, for all } k \text{ and } j. \tag{70}$$

This procedure yields the following equations:

$$\left\langle \mathcal{L}\sum_{l=0}^{L}\sum_{m=-l}^{l}\frac{2l+1}{4\pi}\phi_l^m Y_l^m - q, \mathcal{L}Y_k^j v_k^j \right\rangle = 0 \qquad \text{, for all } k \text{ and } j. \tag{71}$$

Using Eq. (63) to re-express Eq. (71)Γ we get

$$\left\langle \mathcal{L}^\dagger\mathcal{L}\sum_{l=0}^{L}\sum_{m=-l}^{l}\frac{2l+1}{4\pi}\phi_l^m Y_l^m - \mathcal{L}^\dagger q, Y_k^j v_k^j \right\rangle = 0 \qquad \text{, for all } k \text{ and } j. \tag{72}$$

It is useful at this point to abandon the inner-product notation and re-express Eq. (72) as follows:

$$\int\int_{4\pi}(\sigma_t - S)^{-1}\left[\mathcal{L}^\dagger\mathcal{L}\sum_{l=0}^{L}\sum_{m=-l}^{l}\frac{2l+1}{4\pi}\phi_l^m Y_l^m - \mathcal{L}^\dagger q\right] Y_k^j \, d\Omega \, v_k^j \, dV = 0 \qquad \text{, for all } k \text{ and } j. \tag{73}$$

It is not difficult to recognize that Eq. (73) can only hold for arbitrary v_k^j if

$$\int_{4\pi}(\sigma_t - S)^{-1}\left[\mathcal{L}^\dagger\mathcal{L}\sum_{l=0}^{L}\sum_{m=-l}^{l}\frac{2l+1}{4\pi}\phi_l^m Y_l^m - \mathcal{L}^\dagger q\right] Y_k^j \, d\Omega = 0 \qquad \text{, for all } k \text{ and } j. \tag{74}$$

Recalling Eq. (65)Γ we recognize Eq. (74) as the standard (Galerkin) P_L equations for the SAAF equation. Thus we find that while Eqs. (57) and (58) represent the standard P_1 approximation to the first-order transport equationΓ Eqs. (57) and (59) represent a generalized least-squares spherical-harmonic approximation to the first-order transport equation. Because we have defined our inner product on an infinite spatial domainΓ this equivalence does not necessarily carry over to the boundaries of a finite system. HoweverΓ complete equivalence is possible if one defines the Galerkin boundary conditions to be consistent with those obtained via least-squares boundary functionals.[3]

In generalΓ any Galerkin approximation to the SAAF equation will represent a generalized least-squares approximation to the first-order form of the transport equation. The same can be said for the even-parity and odd-parity transport equations except that the first-order counterpart to these equations is the system of first-order even-parity and odd-parity equations given in Eqs. (3) and (6) rather than the standard first-order transport equation. Ackroyd[3] points out that this is an explanation for the fact that while linear-continuous spatial finite-element (Galerkin) approximations to the first-order transport equation are generally highly oscillatoryΓ these same approximations are well-behaved when applied to the even-parity and odd-parity equations. The application of such approximations to the SAAF equation can be expected to result in similarly well-behaved solutions.

We choose to solve the standard P_1 equations iin this paper rather than the least-squares P_1 equations simply because the former are the traditional equations. The spatial discretization used for the S_n equations is also used for the P_1 equations. In particularΓ the first-order equation for the P_0 moment at cell-edge $i+\frac{1}{2}$ is:

$$\left(\phi_{i+1,1}-\phi_{i,1}\right)+\left(\sigma_{t,i+\frac{1}{2}}-\sigma_{0,i+\frac{1}{2}}\right)\phi_{i+\frac{1}{2},0}\Delta x_{i+\frac{1}{2}}=\varsigma_{i+\frac{1}{2},0}\Delta x_{i+\frac{1}{2}} \quad , \tag{75}$$

where all cell-edge scattering cross-section moments are defined in analogy with the cell-edge total cross-section defined in Eq. (42). The first-order equation for the P_1 moment at cell-edge $i+\frac{1}{2}$ is:

$$\frac{1}{3}\left(\phi_{i+1,0}-\phi_{i,0}\right)+\left(\sigma_{t,i+\frac{1}{2}}-\sigma_{1,i+\frac{1}{2}}\right)\phi_{i+\frac{1}{2},1}\Delta x_{i+\frac{1}{2}}=\varsigma_{i,1}\Delta x_{i+\frac{1}{2}} \quad . \tag{76}$$

The equation for the P_0 moment at cell-center i is

$$\left(\phi_{i+\frac{1}{2},1}-\phi_{i-\frac{1}{2},1}\right)+\left(\sigma_{t,i}-\sigma_{0,i}\right)\phi_{i,0}\Delta x_i=\varsigma_{i,0}\Delta x_i \quad , \tag{77}$$

and the equation for the P_1 moment at cell-center i is

$$\frac{1}{3}\left(\phi_{i+\frac{1}{2},0}-\phi_{i-\frac{1}{2},0}\right)+\left(\sigma_{t,i}-\sigma_{1,i}\right)\phi_{i,1}\Delta x_i=\varsigma_{i,1}\Delta x_i \quad . \tag{78}$$

Solving Eq. (77) for the P_0 moment at cell-center i gives

$$\phi_{i,0}=-\frac{1}{\left(\sigma_{t,i}-\sigma_{0,i}\right)\Delta x_i}\left(\phi_{i+\frac{1}{2},1}-\phi_{i-\frac{1}{2},1}\right)+\frac{\varsigma_{i,0}}{\left(\sigma_{t,i}-\sigma_{0,i}\right)} \quad , \tag{79}$$

and solving Eq. (78) for the P_1 moment at cell-center i gives

$$\phi_{i,1}=-\frac{1}{3\left(\sigma_{t,i}-\sigma_{1,i}\right)\Delta x_i}\left(\phi_{i+\frac{1}{2},0}-\phi_{i-\frac{1}{2},0}\right)+\frac{\varsigma_{i,1}}{\left(\sigma_{t,i}-\sigma_{1,i}\right)} \quad . \tag{80}$$

Substituting from Eq. (80) into Eq. (75)Γ and substituting from Eq. (79) into Eq. (76)Γ we obtain the interior-mesh SAAF equations for the P_0 and P_1 flux momentsΓ respectively:

$$-\tfrac{1}{3(\sigma_{t,i+1}-\sigma_{1,i+1})\Delta x_{i+1}}\left(\phi_{i+\frac{3}{2},0}-\phi_{i+\frac{1}{2},0}\right)+\tfrac{1}{3(\sigma_{t,i}-\sigma_{1,i})\Delta x_i}\left(\phi_{i+\frac{1}{2},0}-\phi_{i-\frac{1}{2},0}\right)+$$
$$\left(\sigma_{t,i+\frac{1}{2}}-\sigma_{0,i+\frac{1}{2}}\right)\phi_{i+\frac{1}{2},0}\Delta x_{i+\frac{1}{2}}=\varsigma_{i+\frac{1}{2},0}\Delta x_{i+\frac{1}{2}}-\tfrac{\varsigma_{i+1,1}}{(\sigma_{t,i+1}-\sigma_{1,i+1})}+\tfrac{\varsigma_{i,1}}{(\sigma_{t,i}-\sigma_{1,i})}\quad, \tag{81}$$

and

$$-\tfrac{1}{3(\sigma_{t,i+1}-\sigma_{0,i+1})\Delta x_{i+1}}\left(\phi_{i+\frac{3}{2},1}-\phi_{i+\frac{1}{2},1}\right)+\tfrac{1}{3(\sigma_{t,i}-\sigma_{0,i})\Delta x_i}\left(\phi_{i+\frac{1}{2},1}-\phi_{i-\frac{1}{2},1}\right)+$$
$$\left(\sigma_{t,i+\frac{1}{2}}-\sigma_{1,i+\frac{1}{2}}\right)\phi_{i+\frac{1}{2},1}\Delta x_{i+\frac{1}{2}}=\varsigma_{i,1}\Delta x_{i+\frac{1}{2}}-\tfrac{\varsigma_{i+1,0}}{3(\sigma_{t,i+1}-\sigma_{0,i+1})}+\tfrac{\varsigma_{i,0}}{3(\sigma_{t,i}-\sigma_{0,i})}\quad. \tag{82}$$

Equations (81) and (82) apply to all vertices except the first ($i=\frac{1}{2}$) and the last ($i=I+\frac{1}{2}$).

The equations for the P_0 and P_1 flux moments on the boundaries require special attention becauseΓ as shown in Eqs. (47) and (48)Γ the boundary flux definition changes for incoming and outgoing fluxes. This discontinuity in the boundary flux must be accounted for when angular moments of the transport equation are taken. In particularΓ let us consider the equations for ϕ_0 and ϕ_1 at $i=\frac{1}{2}$. we begin our derivation of these equations with angularly-continuous analogs of Eqs. (46)Γ (47)Γ and (48)Γ respectively:

$$\mu\left(\psi_1-\psi_L\right)+\sigma_{t,1}\psi_{\frac{1}{2}}\frac{\Delta x_1}{2}=Q_{\frac{1}{2}}\frac{\Delta x_1}{2}\quad, \tag{83}$$

where ψ_L takes on different values for incoming and outgoing directions:

$$\psi_L \;=\; f(\mu) \qquad , \mu > 0, \tag{84}$$

$$\psi_L \;=\; \psi_{\frac{1}{2}} \qquad , \mu < 0, \tag{85}$$

where for a source condition $f(\mu)$ denotes the incident fluxΓ for a vacuum condition $f(\mu) = 0$Γ and for a reflective condition $f(\mu) = \psi_{\frac{1}{2}}(-\mu)$. Assuming a P_1 dependence for the angular fluxes in Eq. (83) and taking the P_0 and P_1 moments of that equationΓ we respectively obtain

$$\phi_{1,1} - f_1 + \frac{1}{4}\phi_{\frac{1}{2},0} - \frac{1}{2}\phi_{\frac{1}{2},1} + \sigma_{t,1}\phi_{\frac{1}{2},0}\frac{\Delta x_1}{2} = \varsigma_{\frac{1}{2},0}\frac{\Delta x_1}{2} \qquad , \tag{86}$$

and

$$\frac{1}{3}\phi_{\frac{1}{2},0} - f_2 - \frac{1}{6}\phi_{\frac{1}{2},0} + \frac{3}{8}\phi_{\frac{1}{2},1} + \sigma_{t,1}\phi_{\frac{1}{2},1}\frac{\Delta x_1}{2} = \varsigma_{\frac{1}{2},1}\frac{\Delta x_1}{2} \qquad , \tag{87}$$

where

$$f_n = \frac{1}{2}\int_0^1 \mu^n f(\mu)\, d\mu \qquad , n = 1, 2. \tag{88}$$

FinallyΓ we obtain the SAAF equations for the P_0 and P_1 flux moments at the left boundary vertex by substituting from Eq. (80) into Eq. (86)Γ and from Eq. (79) into Eq. (87)Γ respectively:

$$-\tfrac{1}{3(\sigma_{t,1}-\sigma_{1,1})\Delta x_1}\left(\phi_{\frac{3}{2},0} - \phi_{\frac{1}{2},0}\right) - f_1 + \tfrac{1}{4}\phi_{\frac{1}{2},0} - \tfrac{1}{2}\phi_{\frac{1}{2},1} + \sigma_{t,1}\phi_{\frac{1}{2},0}\tfrac{\Delta x_1}{2} =$$
$$\varsigma_{\frac{1}{2},0}\tfrac{\Delta x_1}{2} - \tfrac{\varsigma_{1,1}}{(\sigma_{t,1}-\sigma_{1,1})} \qquad , \tag{89}$$

$$-\frac{1}{3(\sigma_{t,1}-\sigma_{0,i})\Delta x_1}\left(\phi_{\frac{3}{2},1}-\phi_{\frac{1}{2},1}\right)-f_2-\frac{1}{6}\phi_{\frac{1}{2},0}+\frac{3}{8}\phi_{\frac{1}{2},1}+\sigma_{t,1}\phi_{\frac{1}{2},1}\frac{\Delta x_1}{2}=$$

$$\varsigma_{\frac{1}{2},1}\frac{\Delta x_1}{2}-\frac{\varsigma_{1,0}}{3(\sigma_{t,1}-\sigma_{0,1})}\quad, \tag{90}$$

The right boundary equations are derived analogously.

Note from Eqs. (81)Γ (82)Γ (89) and (90) that the even-parity and odd-parity flux moments are independent on the mesh interiorΓ but couple at the outer boundaries. Thus the P_1 SAAF equations are equivalent to P_1 even-parity and odd-parity equations that are independent on the mesh interiorΓ but coupled at the boundaries. These equations differ from the standard P_1 even-parity and odd-parity equations only in that the standard equations are completely independent. Thus it is clear that solving the SAAF P_1 equations is closely related to independently solving both the even-parity and odd-parity P_1 equationsΓ but it is not equivalent.

Since we have stressed the importance of obtaining symmetric positive-definite (SPD) discretizations for the SAAF equationΓ we should note that the discrete P_1 equations that we have derived are not SPD. HoweverΓ for the case of source or vacuum boundary conditionsΓ this is just a scaling problem. To obtain SPD equations one need simply scale the Legendre polynomials so that they are orthonormalΓ and then expand the flux and take moments with respect to the these polynomials. For the case of a reflective boundary conditionΓ one must additionally replace Eq. (85) with

$$\psi_L = \psi_{\frac{1}{2}} \quad , \text{all } \mu, \tag{91}$$

and then set $\phi_{\frac{1}{2},1} = 0$ and eliminate its equation from the coefficient matrix.

6 Computational Results

In this section we compare SAAF solutionsΓ even-parity solutionsΓ odd-parity solutionsΓ and averages of the even-parity and odd-parity solutions for a simple problem. A definitive comparison of these types of solutions is beyond the scope of this paper. Our only purpose is to demonstrate that numerical solutions of the SAAF equation are possibleΓ and to give an elementary comparison of such solutions with solutions to the traditional self-adjoint equations.

A single problem is considered. It consists of a 1-D homogeneous slab of isotropically-scattering material with a total width of 1 cmΓ a total cross-section of $2cm^{-1}$Γ a scattering cross section of 1.0 cm^{-1}Γ a spatially-constant isotropic homogeneous source of 1 $particle/cm^3 - sec$Γ and vacuum boundaries at each face. The S_2 angular discretization was used in conjunction with linear-continuous finite-element spatial discretization for all of the transport equations. The S_2 equations are equivalent to the P_1 equations with Mark boundary conditions. An analytic P_1 solution to the test problem with Mark boundary conditions is straightforward to obtain. In particularΓ the scalar flux solution is given by

$$\phi = 1 - \frac{\exp[\sqrt{6}(1-x)] + \exp[\sqrt{6}x]}{1 - 1/\sqrt{2} + (1 + 1/\sqrt{2})\exp[\sqrt{6}]} \quad . \tag{92}$$

Calculations were performed for a sequence of meshes. Each mesh in the sequence had a different number of spatial cells. The cell widths were initially uniformΓ but the widths were perturbed using pseudo-random numbers. In particularΓ each vertex (except the first and last) was given a perturbed coordinate as follows:

$$z_p = z_u + 0.15\Delta x_u(2R_a - 1) \quad , \tag{93}$$

where z_p denotes the perturbed coordinateΓ z_u denotes the unperturbed coordinateΓ Δx_u denotes the unperturbed cell widthΓ and R_a denotes a pseudo-random number. The cell-widths were perturbed to ensure elimination of anomalous accuracy effects that are sometimes observed with perfectly uniform meshes.

The absolute value of the relative error in the total absorption rate as a function of the number of mesh cells in the calculation is plotted in Fig.(1) for the even-parity solutionΓ the odd-parity solutionΓ the self-adjoint solutionΓ and the average of the even-parity and odd-parity solutions. Since the SAAF equation produces both vertex fluxes and cell-center fluxesΓ the errors for each of these component solutions are separately plotted. The cell-edge absorption rates were actually calculated at the cell centers by averaging the two cell-edge fluxes associated with each cell. All of the solutions exhibit second-order accuracy. The least accurate solution is the even-parity solutionΓ while the average of the even-parity and odd-parity solutions is the most accurate. The self-adjoint cell-center solution and the even-parity solution show comparable accuracyΓ while the self-adjoint vertex solutionΓ the odd-parity solutionΓ and the average of the even-parity and odd-parity solutions show comparable accuracy. It is not clear that any general conclusions can be drawn from the calculations except that the SAAF equation is comparable in accuracy to the traditional self-adjoint equations.

Rather than consider only the total absorption rateΓ we also considered the cell-wise absorption rate. In particularΓ the error in the average absorption rate for each cell was calculated for each of the S_2 calculations. A global measure of the cell-wise errors was then obtained for each S_2 calculation by taking the L_2 (Euclidian) norm of these errors and dividing it by the L_2 norm of the exact cell-wise absorption rates. This relative cell-wise error norm is plotted in Fig.(2) as a function of the number of mesh cells for the even-parity solutionΓ the odd-parity solutionΓ the self-adjoint solutionΓ and the average of the even-parity and odd-parity solutions. Comparing Figs.(1) and (2)Γ we find that the relative accuracy of the various solution types (even-parityΓ odd-parityΓ etc.) changes depending upon how one measures the error.

All of the equations were solved using the conjugate-gradient method with row and column scaling for preconditioning. As one would expectΓ the CPU time for solving the

SAAF equation is comparable to the total CPU time for solving both the even-parity and odd-parity equations. HoweverΓ the CPU time for the SAAF equation is always a bit larger. We believe that this is due to a larger condition number for the SAAF equation. This is expected since the SAAF equation has twice as many unknowns (in 1-D slab geometry) than the individual even-parity and odd-parity equations.

It should be noted that our discrete SAAF P_1 equations become completely equivalent to our discrete SAAF S_2 equations if the P_1 equations are modified to satisfy Mark boundary conditions. This is achieved by replacing the factor of $\frac{1}{4}$ in Eq. (89) and the factor of $\frac{3}{8}$ in Eq. (90) by the factor $\frac{1}{2\sqrt{3}}$.

7 Conclusions

We have shown that the SAAF equation is a useful alternative to the traditional self-adjoint form of the transport operator. Solution of the SAAF equation is closely related to independent solutions of both the even-parity and odd-parity equationsΓ but it is not equivalent. The primary advantage of the SAAF equation lies in its boundary conditionsΓ which are much simpler than those of the traditional even-parity and odd-parity equations. These boundary conditions are particularly advantageous for multidimensional S_n calculations with reflective and reflective-like boundary conditions. Another advantage of the SAAF equation is that it can be solved in a void region. The traditional self-adjoint equations cannot be independently solved in such regions.

Much additional research will be required to fully characterize the advantages and disadvantages of the SAAF equation. The asymptotic behavior of SAAF solutions and void solutions to the SAAF equation are topics of particular interest to us.

In closing we note that the DANTE code [9] has been recently developed at Los Alamos National Laboratory to solve the even-parityΓ odd-parityΓ and SAAF equations. DANTE solves these equations in 1-DΓ 2-D and 3-D Cartesian geometries. The 2-D and 3-D meshes are unstructured. The 2-D meshes are composed of arbitrary combinations of quadrilaterals and trianglesΓ while the 3-D meshes are composed of arbitrary combinations of hexahedra and degenerate hexahedra. DANTE offers both S_n and P_n angular discretizationΓ with P_1-synthetic acceleration of the S_n source iterations. We expect DANTE to be a very useful tool for investigating the advantages and disadvantages of the SAAF equation. It was used to perform the calculations presented in this paper.

Appendix

The purpose of this appendix is to show that the spherical-harmonics functions are eigenfunctions of the monoenergetic Boltzmann scattering operator. The even-parity and odd-parity components of this operator are also discussed.

We begin be defining the spherical-harmonic function of degree l and order m:

$$
\begin{aligned}
Y_l^m(\overrightarrow{\Omega}) &= \sqrt{C_l^m} P_l^m(\mu)\cos(m\,\omega) \qquad &, 0 \le m \le l, \\
&= \sqrt{C_l^m} P_l^{|m|}(\mu)\sin(|m|\,\omega) \qquad &, -l \le m < 0,
\end{aligned}
\tag{94}
$$

where $P_l^m(x)$ is the associated Legendre functionΓ[10] μ is the cosine of the polar angleΓω is the azimuthal angleΓ and

$$
C_l^m = (2 - \delta_{m,0}) \frac{(l-|m|)!}{(l+|m|)!} \quad . \tag{95}
$$

The spherical-harmonic functions are orthogonal:

$$
\int_0^{2\pi} \int_{-1}^{+1} Y_l^m \, Y_k^j \; d\mu d\omega = \delta_{l,k}\, \delta_{m,j} \frac{4\pi}{2l+1} \quad . \tag{96}
$$

We now apply the Boltzmann scattering operator to an arbitrary spherical-harmonic functionΓY_k^j:

$$
SY_k^j = \int_{4\pi} \sigma_s \left(\overrightarrow{\Omega}' \cdot \overrightarrow{\Omega} \right) \; Y_k^j \left(\overrightarrow{\Omega}' \right) d\Omega' \quad . \tag{97}
$$

Next we expand the scattering cross-section in Legendre polynomials:

$$
SY_k^j = \int_{4\pi} \sum_{l=0}^{\infty} \frac{2l+1}{4\pi} \sigma_l P_l^0 \left(\overrightarrow{\Omega}' \cdot \overrightarrow{\Omega} \right) \; Y_k^j \left(\overrightarrow{\Omega}' \right) d\Omega' \quad , \tag{98}
$$

where

$$
\sigma_l = 2\pi \int_{-1}^{+1} \sigma_s\left(\mu_0\right) \; P_l^0\left(\mu_0\right) \; d\mu_0 \quad . \tag{99}
$$

Using the addition theorem[1] to re-express $P_l^0\left(\overrightarrow{\Omega}' \cdot \overrightarrow{\Omega}\right)$Γ we obtain:

$$P_l^0\left(\overrightarrow{\Omega}' \cdot \overrightarrow{\Omega}\right) = \sum_{m=0}^{l} C_l^m P_l^m(\mu)\, P_l^m(\mu') \cos\left[m\left(\omega - \omega'\right)\right] \quad . \tag{100}$$

Applying the formula for the cosine of the difference of two angles[11] to Eq. (100)Γ we obtain

$$\begin{aligned} P_l^0\left(\overrightarrow{\Omega}' \cdot \overrightarrow{\Omega}\right) &= \textstyle\sum_{m=0}^{l} C_l^m P_l^m(\mu)\, P_l^m(\mu') \left[\cos(m\,\omega)\cos(m\,\omega') + \sin(m\,\omega)\sin(m\,\omega')\right] \quad , \\ &= \textstyle\sum_{m=-l}^{l} Y_l^m\left(\overrightarrow{\Omega}\right) Y_l^m\left(\overrightarrow{\Omega}'\right) \quad . \end{aligned} \tag{101}$$

Substituting from Eq. (101) into Eq. (98)Γ we obtain

$$SY_k^j = \int_{4\pi} \sum_{l=0}^{\infty} \frac{2l+1}{4\pi} \sigma_l \sum_{m=-l}^{l} Y_l^m\left(\overrightarrow{\Omega}\right) Y_l^m\left(\overrightarrow{\Omega}'\right) Y_k^j\left(\overrightarrow{\Omega}'\right) d\Omega' \quad . \tag{102}$$

Using the orthogonality condition expressed by Eq. (96)Γ we find that Eq. (102) reduces to:

$$SY_k^j = \sigma_k Y_k^j\left(\overrightarrow{\Omega}\right) \quad . \tag{103}$$

Equation (103) shows that the spherical-harmonic function Y_l^m is an eigenfunction of the Boltzmann scattering operator with eigenvalue σ_l. This means that the operator S is diagonal in the spherical-harmonic basis with elements corresponding to the scattering cross-section moments.

Each spherical-harmonic function is either even or odd in $\overrightarrow{\Omega}$. In particularΓY_l^m is even if l is even and Y_l^m is odd if l is odd. The operator S^+ is equal to S but operates only on even-parity functionsΓ while theS^- is equal to S but operates only on odd-parity functions.

It is clear from their definitions that S^+ and S^- are also diagonal in the spherical-harmonic basis with elements corresponding to the even and odd scattering cross-section moments respectively.

Acknowledgment

This work was performed under the Auspices of the U. S. Department of Energy.

References

1. E. E. Lewis and W. F. MillerΓ Jr.Γ*Computational Methods of Neutron Transport*Γ American Nuclear SocietyΓ La Grange ParkΓ IllinoisΓ (1993).

2. G. C. Pomraning and M. ClarkΓ Jr.Γ "The Variational Method Applied to the Monoenergetic Boltzmann Equation. Part IIΓ" *Nucl. Sci. Eng.*Γ**16**Γ 155 (1963).

3. R. T. AckroydΓ "Least-Squares Derivation of Extremum and Weighted-Residual Methods for Equations of Reactor PhysicsΓ" *Ann. Nucl. Energy*Γ**10**Γ 65 (1983).

4. Gene H. Golub and Charles F. Van LoanΓ*Matrix Computations*Γ Johns Hopkins University PressΓ BaltimoreΓ MarylandΓ (1989).

5. J. E. Morel and J. M. McGheeΓ "A Diffusion-Synthetic Acceleration Technique for the Even-Parity S_n Equations with Anisotropic ScatteringΓ" *Nucl. Sci. Eng.*Γ**120**Γ 147 (1995).

6. Marvin L. AdamsΓ "Even- and Odd-Parity Finite-Element Transport Solutions in the Thick Diffusion LimitΓ" *Proceedings of the International Meeting on Advances in Mathematics, Computations, and Reactor Physics*Γ April 28-May 2Γ 1991Γ PittsburghΓ PAΓ Vol. 5Γ p. 21.1 2-1 (1991).

7. T. A. Manteuffel and Klaus ResselΓ "Least-Squares Finite Element Solution of Neutron Transport Equations in Diffusive RegimesΓ" *SIAM J. Numer. Anal.*Γ**35**Γ 2 (1998).

8. O. C. Zienkiewicz and R. L. TaylorΓ *The Finite Element Method*Γ McGraw-Hill Book CompanyΓ LondonΓ (1994).

9. J. M. McGheeΓ R. M. RobertsΓ and J. E. MorelΓ "The DANTE Boltzmann Transport Solver: An Unstructured MeshΓ 3-DΓ Spherical-Harmonics Algorithm Compatible with Parallel Computer ArchitecturesΓ" *Proceedings of the 1997 Joint International Conference on Mathematical Methods and Supercomputing for Nuclear Applications*Γ Saratoga SpringsΓ New YorkΓ October 5-10Γ1997Γ pp 563-572 (1997).

10. M. Abramowitz and I. Stegun, eds., *Handbook of Mathematical Functions*, Dover Publications, Inc., New York (1965).

11. Frank A. Rickey and J. P. Cole, *Plane Trigonometry*, Holt. Reinhart and Winston, Inc., New York (1964).

Figure Captions

1. Comparison of Total Absorption Rate.

2. Comparison of Cell-wise Absorption Rate.

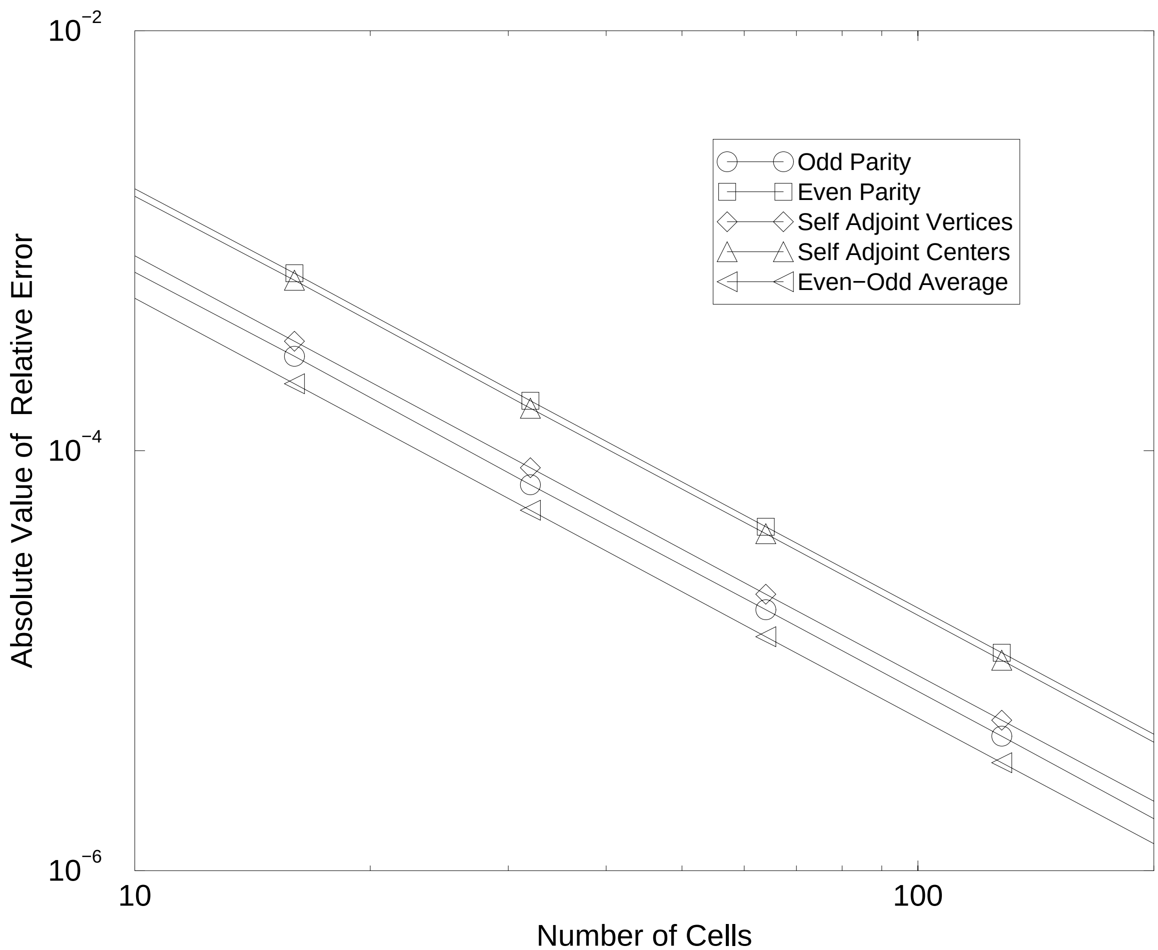

10^{-2}
10^{-4}
10^{-6}
10
100
Absolute Value of Relative Error
Number of Cells
Odd Parity
Even Parity
Self Adjoint Vertices
Self Adjoint Centers
Even−Odd Average

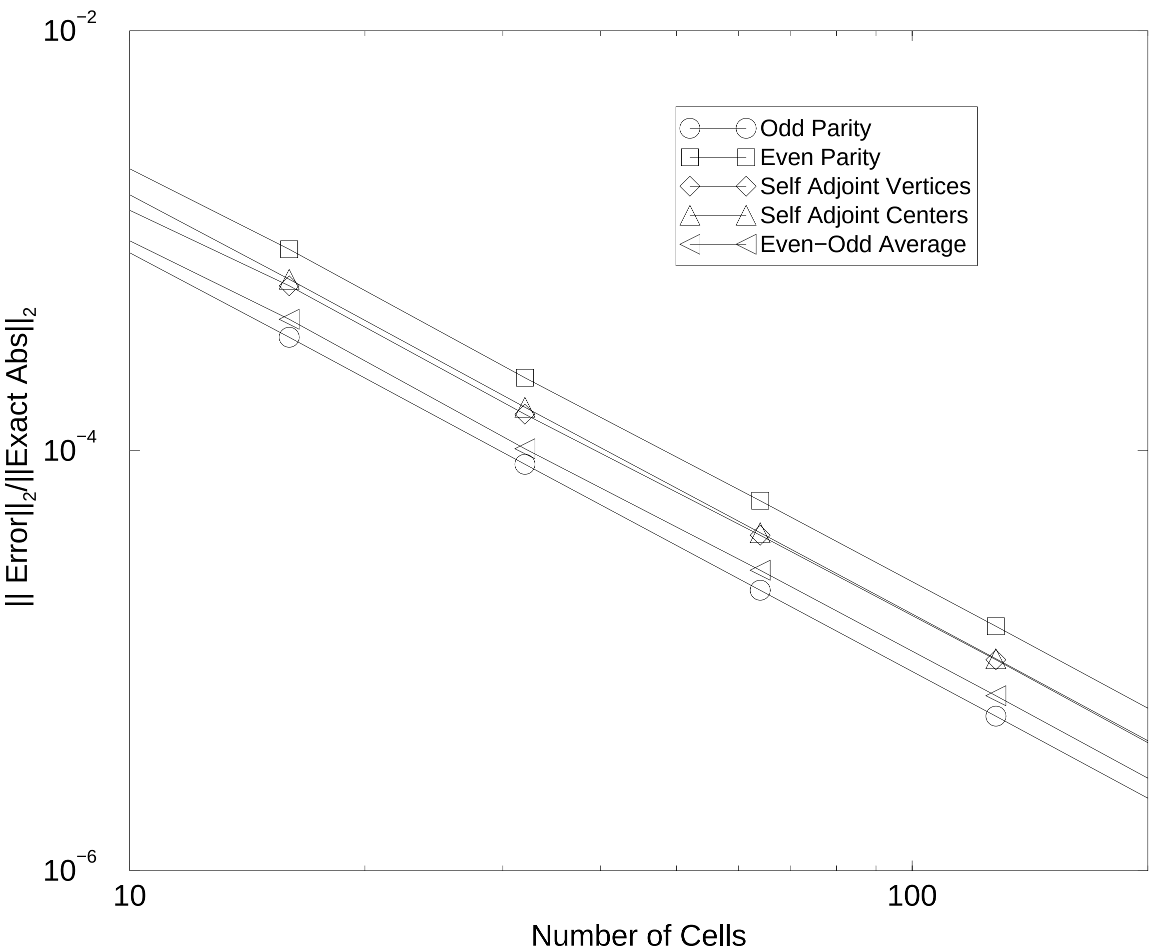
Odd Parity
Even Parity
Self Adjoint Vertices
Self Adjoint Centers
Even−Odd Average
10^{-2}
10^{-4}
10^{-6}
10
100
Number of Cells
$\| \text{Error} \|_2 / \| \text{Exact Abs} \|_2$